HHS Public Access

Author manuscript

Circ Arrhythm Electrophysiol. Author manuscript; available in PMC 2021 July 01.

Published in final edited form as:

Circ Arrhythm Electrophysiol. 2020 July ; 13(7): e008210. doi:10.1161/CIRCEP.119.008210.

Machine Learning of 12-lead QRS Waveforms to Identify Cardiac Resynchronization Therapy Patients with Differential Outcomes

Albert K. Feeny, BS[1], **John Rickard, MD, MPH**[2], **Kevin M. Trulock, MD**[2], **Divyang Patel, MD**[2], **Saleem Toro, MD**[2], **Laurie Ann Moennich, MPH**[2], **Niraj Varma, MD, PhD**[1,2], **Mark J. Niebauer, MD, PhD**[1,2], **Eiran Z. Gorodeski, MD, MPH**[1,2], **Richard A. Grimm, DO**[1,2], **John Barnard, PhD**[1,3], **Anant Madabhushi, PhD**[4,5,*], **Mina K. Chung, MD**[1,2,6,*]

[1]Cleveland Clinic Lerner College of Medicine, Case Western Reserve University

[2]Dept of Cardiovascular Medicine, Heart and Vascular Institute, Cleveland Clinic

[3]Dept of Quantitative Health Sciences, Lerner Research Institute, Cleveland Clinic

[4]Dept of Biomedical Engineering, Case Western Reserve University

[5]Louis Stokes Cleveland Veterans Administration Medical Center, Cleveland, OH

[6]Dept of Cardiovascular and Metabolic Sciences, Lerner Research Institute, Cleveland Clinic

Abstract

Background—Cardiac resynchronization therapy (CRT) improves heart failure outcomes but has significant non-response rates, highlighting limitations in ECG selection criteria: QRS duration (QRSd) ≥150 ms and subjective labeling of left bundle branch block (LBBB). We explored unsupervised machine learning of ECG waveforms to identify CRT subgroups that may differentiate outcomes beyond QRSd and LBBB.

Methods—We retrospectively analyzed 946 CRT patients with conduction delay. Principal components analysis (PCA) dimensionality reduction obtained a two-dimensional representation of pre-CRT 12-lead QRS waveforms. *K*-means clustering of the two-dimensional PCA representation of 12-lead QRS waveforms identified two patient subgroups (QRS PCA groups). Vectorcardiographic QRS area was also calculated. We examined two primary outcomes: (1) composite endpoint of death, left ventricular assist device, or heart transplant, and (2) degree of echocardiographic left ventricular ejection fraction (LVEF) change after CRT.

Correspondence: Mina Chung, MD, Dept Cardiovascular Medicine, Heart and Vascular Institute, Cleveland Clinic, 9500 Euclid Avenue, J2-2, Cleveland, OH 44195, Tel: 216-444-2290, chungm@ccf.org.
*Co-Senior Authors

Disclosures: Dr. Rickard has been a speaker for Boston Scientific and a consultant for Medtronic. Dr. Varma reports consulting fees and honoraria from St. Jude Medical, Boston Scientific, Sorin, Biotronik, and Medtronic. Dr. Niebauer reports research support from Biosense Webster, Biotronik, Boston Scientific, Medtronic, St. Jude Medical, and Sorin. Dr. Gorodeski reports research support and consulting fees from Abott. Dr. Madabhushi is an equity holder in Elucid Bioimaging and Inspirata, is a scientific advisory consultant for Inspirata, has been a scientific advisory board member for Inspirata, Astrazeneca and Merck, and has sponsored research agreements with Philips and Inspirata. His technology has been licensed to Elucid Bioimaging and Inspirata. He is involved in NIH grants with PathCore and Inspirata. Dr. Chung serves on the steering committee for and has spoken at conferences for EPIC Alliance, a forum for networking and mentoring of women in cardiac electrophysiology sponsored by Biotronik, but declines honoraria from device companies. All other authors have no relevant relationships to disclose.

Results—Compared to QRS PCA Group 2 (*n*=425), Group 1 (*n*=521) had lower risk for reaching the composite endpoint (HR 0.44, 95% CI, 0.38–0.53, p<0.001) and experienced greater mean LVEF improvement (11.1±11.7% vs. 4.8±9.7%, p<0.001), even among LBBB patients with QRSd ≥150 ms (HR 0.42, 95% CI, 0.30–0.57, p<0.001; mean LVEF change 12.5±11.8% vs. 7.3±8.1%, p=0.001). QRS area also stratified outcomes but had significant differences from QRS PCA groups. A stratification scheme combining QRS area and QRS PCA group identified LBBB patients with similar outcomes to non-LBBB patients (HR 1.32, 95% CI: 0.93–1.62; difference in mean LVEF change: 0.8%, 95% CI: −2.1%−3.7%). The stratification scheme also identified LBBB patients with QRSd <150 ms with comparable outcomes to LBBB patients with QRSd ≥150 ms (HR: 0.93, 95% CI: 0.67–1.29; difference in mean LVEF change: −0.2%, 95% CI: −2.7% −3.0%).

Conclusions—Unsupervised machine learning of ECG waveforms identified CRT subgroups with relevance beyond LBBB and QRSd. This method may assist in objective classification of bundle branch block morphology in CRT.

Keywords

ECG; cardiac resynchronization therapy; heart failure; machine learning

Journal Subject Terms:

Arrhythmias; Electrophysiology; Electrocardiology (ECG); Pacemaker

Introduction

Cardiac resynchronization therapy (CRT) improves outcomes in heart failure patients with ventricular dyssynchrony[1–3–], but 30–50% of patients have apparent lack of response to treatment[4]. Prolonged QRS duration (QRSd) and left bundle branch block (LBBB) on 12-lead electrocardiogram (ECG) are key guideline criteria for patient selection[5] but have limitations. QRSd is insensitive for left ventricular (LV) activation delay in non-LBBB[6] and is affected by LV dimension in LBBB[7]. LBBB is one of the strongest CRT selection criteria and predictors of CRT response[8], but has been plagued by unstandardized definitions, subjective assessment[9], and variable clinical judgement[10].

Several ECG metrics have purported improved CRT response prediction, including strict LBBB criteria[9], QRS frequency content[11], intrinsicoid deflection onset[12], LV activation time[13], sum of absolute QRS-T integral[14], and QRS area[15,16]. However, ECGs may be more comprehensively evaluated with machine learning to improve CRT ECG criteria[17].

Dimensionality reduction is a machine learning approach to create low-dimensional representations from the original high-dimensional data, and unsupervised clustering can identify relevant groups from natural data variations[18,19]. Cikes *et al.* used such techniques to integrate clinical parameters with echocardiographic LV traces to identify heart failure phenogroups that may assist CRT patient selection[20]. We present an approach to extend these concepts toward conduction delay manifestations on ECG waveforms.

Principal components analysis (PCA) is a linear dimensionality reduction method, and *k*-means clustering is a method of partitioning data based on cluster means. We hypothesized that 1) 12-lead QRS waveform analysis using PCA and *k*-means clustering could identify CRT patient subgroups with differential primary outcomes of survival and reverse remodeling defined by echocardiographic LV ejection fraction (LVEF) change, and 2) these subgroups would discriminate outcomes within subgroups defined by subjective LBBB and QRSd. In this study, patients with echocardiographic and survival outcomes were used to derive QRS PCA groups from the PCA representation of 12-lead QRS patterns. Primary outcomes of the QRS PCA groups were assessed among subgroups defined by LBBB, QRSd, and QRS area and evaluated in internal validation cohorts. We then determined outcomes associated with combinations of QRS morphology and objectively defined QRS area and QRS PCA groups.

Methods

This study was approved by the Institutional Review Board of the Cleveland Clinic. Because of the sensitive nature of the data collected for this study, requests to access the dataset from qualified researchers trained in human subject confidentiality protocols may be sent to the corresponding author.

Study population

This was a retrospective cohort study of patients at the Cleveland Clinic (Figure 1) receiving CRT implants from 2003–2012 with long-term outcomes collected, as well as a separate CRT-HF registry at the Cleveland Clinic who received CRT implantation between 2017–2018. The CRT-HF registry was established to study a novel, multidisciplinary approach toward post-CRT care via a 6-month post-implant visit with imaging, heart failure, ECG, and device assessment[21]. Compared to the remainder of the study population, CRT-HF patients were more contemporary and did not have long-term survival outcomes recorded. CRT-HF patients did not have differing inclusion criteria, and did not receive differential post-CRT care prior to the 6-month visit when echocardiographic response was recorded. We included patients whose pre-implant ECG demonstrated native conduction delay adjudicated as previously described[8] (LBBB, right bundle branch block (RBBB), or non-specific intraventricular conduction delay (IVCD)), and excluded patients with narrow (QRSd <120 ms) or paced QRS. LBBB was defined as QRSd ≥120 ms, monophasic QS or rS complex in V1, and monophasic R-wave in V6[8].

The study population consisted of Primary, Survival Validation, and Echo Validation Cohorts (Figure 1). The Primary Cohort included patients from 2003–2012 with pre- and post-implant echocardiographic LVEF measurements and survival data. The Survival Validation Cohort consisted of patients from 2003–2012 that had survival but not LVEF data. The Echo Validation Cohort consisted of CRT-HF patients, who had LVEF but not survival data.

ECG analysis

The most recent digital 10-second 12-lead ECGs prior to CRT implant were exported from the Muse System (General Electric Healthcare, Little Chalford, UK). The median QRS

complex from each lead for each patient was obtained using custom software[14,22] in MATLAB 2018b (MathWorks, Natick, MA) (Supplemental Methods). QRS area was calculated from the reconstructed vectorcardiogram using the Kors method as previously described[23].

Unsupervised machine learning to identify QRS PCA groups

Unsupervised machine learning using dimensionality reduction and clustering is depicted in Figure 2. A feature vector was constructed for each patient, composed of the median QRS waveform from each lead and QRSd. In the Primary Cohort, PCA was performed on the feature vectors across all patients to obtain a low-dimensional representation of each patient's QRS waveforms. Two groups were identified using *k*-means clustering on the low-dimensional QRS PCA representation. Technical details are provided in the Supplemental Methods.

Outcomes

Primary outcomes for this study were (1) a composite endpoint of death, heart transplant, or placement of left ventricular assist device (LVAD) and (2) degree of LVEF change following CRT implant. Secondary outcomes included changes in LV end-diastolic diameter (LVEDD) and end-systolic diameter (LVESD), mitral regurgitation (MR)), and New York Heart Association (NYHA) functional class. Survival was determined from the US Social Security Death Index and electronic medical records review. The pre-implant echocardiogram was the last prior to implantation. In the Primary Cohort, the post-implant echocardiogram was closest to 1-year follow-up[8]. In the Echo Validation Cohort, the post-implant echocardiogram was performed at 6-month follow-up. Patients with a post-implant echocardiogram within 60 days after implant were excluded from echocardiographic comparisons.

To assess relevance of groups identified from the QRS PCA representation, we compared primary outcomes in the entire cohort and in subgroups defined by LBBB, QRSd, and QRS area. QRS area was selected for comparison because it enhanced CRT response prediction from QRSd, LBBB, and strict LBBB[15,23,24]. QRS area groups were defined by a cutoff of ≤95 μVs[16].

Evaluation of the QRS PCA representation

The PCA representation was interpreted via mapping vectors **w** (Supplemental Methods Equation 1), revealing how the QRS PCA representation was determined in a given dimension. Stability of the QRS PCA representation was evaluated (Supplemental Methods). Outcomes of the two groups identified by clustering of the QRS PCA representation were compared in the entire Primary Cohort and within subgroups defined by LBBB and QRSd ≥150 ms. QRS area groups were also compared. The effect of 12-lead analysis versus reduced-lead analysis was examined (Supplemental Methods). Outcome discrimination from PCA compared to nonlinear dimensionality reduction methods was quantified, as well as the effect of ECG input with and without QRSd and QRS area prior to PCA and clustering (Supplemental Methods).

Because the QRS PCA representation was empirically derived, generalizability to data outside of the Primary Cohort was assessed. Patients in validation cohorts were assigned QRS PCA group using the same mapping vectors and clusters derived from the Primary Cohort (Supplemental Methods). Cluster stability was assessed by independently repeating the PCA and clustering process in the validation cohorts (Supplemental Methods). Survival free from the composite endpoint and LVEF change were assessed on the Survival Validation and Echo Validation Cohorts, respectively. Multivariable models containing age and baseline characteristics that are known predictors of CRT outcomes and significantly different between the QRS PCA groups were constructed. The effect of combining QRSd, LBBB, QRS PCA representations, QRS area, and common clinical variables[25] in supervised learning models was evaluated (Supplemental Methods). Finally, interaction between LV lead location and QRS PCA groups was assessed (Supplemental Methods).

Stratifying QRS morphology by QRS PCA group and QRS area

Both QRS PCA group and QRS area offered greater stratification of outcomes in LBBB than QRSd. We then assessed how CRT outcomes differed when QRS morphology was stratified by combinations of QRS area and QRS PCA groups, rather than by QRSd. Four subgroups were defined by QRS morphology and QRSd to represent current guidelines: (1) LBBB and QRSd ≥150 ms (2) LBBB and QRSd <150 ms (3) non-LBBB and QRSd ≥150 ms, and (4) non-LBBB and QRSd <150 ms. Primary outcomes were assessed in each group, using non-LBBB and QRSd <150 ms as reference for comparisons.

Next, four subgroups were defined by using QRS area and QRS PCA representation to stratify QRS morphology: (1) LBBB, and either QRS area >95 μVs or QRS PCA Group 1 (2) LBBB, QRS area ≤95 μVs, and QRS PCA Group 2 (3) non-LBBB, and either QRS area >95 μVs or QRS PCA Group 1, and (4) non-LBBB, QRS area ≤95 μVs, and QRS PCA Group 2. Primary outcomes were examined in subgroups, using non-LBBB, QRS area ≤95 μVs, and QRS PCA Group 2 as reference for comparisons.

Statistical analysis

Group differences were assessed in categorical variables with the chi-squared test, in normally distributed continuous variables with the two-sample *t*-test, and in non-normally distributed continuous variables with the Wilcoxon rank-sum test. Multivariable linear regression was used to assess LVEF change. Kaplan-Meier curves were used to visualize survival. Cox proportional hazards models were used to compare event-free survival between groups for the composite endpoint. Unless stated otherwise, all Cox models reported were univariable. A multivariable Cox model was used when comparing outcomes of the QRS PCA groups on the entire study cohort, and included age as well as baseline clinical characteristics that are known predictors of CRT outcomes and significantly different between the QRS PCA groups (sex, ischemic cardiomyopathy, QRSd, LBBB, history of atrial fibrillation, creatinine, presence of end-stage renal disease on hemodialysis). Proportional hazard assumptions were verified by testing for independence between scaled Schoenfield residuals and time for each covariate. Age at time of implant violated this assumption, with increasing residuals over time. Since the objective was not to precisely model the effect of age over time, but rather to evaluate for a confounding impact on the

significance of the QRS PCA groups, age was modeled as a time-independent covariate. Two-sided $p<0.05$ was considered significant. Survival curves were generated in MATLAB and statistics were calculated with R 3.5.1 (R Foundation, Vienna, Austria) using packages "survival" and "tableone."

Results

946 patients were analyzed in the study (Table 1). 539 patients comprised the Primary Cohort, 301 patients comprised the Survival Validation Cohort, and 106 patients comprised the Echo Validation Cohort (Figure 1). Median time from baseline ECG to CRT implant was 15.7 [interquartile range: 4–42.5] days.

Evaluation of QRS PCA representation

Figure 2 shows *k*-means clustering of the QRS PCA representation, retaining two PCA dimensions (Supplemental Figure 1). Clustering was driven by dimension 1, termed the QRS PCA score, which was obtained via the mapping vector (Figure 2). Higher PCA scores had greater voltage amplitudes and patterns consistent with LBBB. The QRS PCA score had stable configuration (Supplemental Figure 2).

K-means clustering identified two groups from the QRS PCA representation. In the Primary Cohort, QRS PCA Group 1 had a higher QRS PCA score and had better event-free survival and greater LVEF improvement than Group 2 (HR 0.44, 95% CI [0.35–0.55], p<0.001; mean LVEF change 11.4±12.1% vs. 4.6±10.0%, p<0.001). Similar outcome stratification occurred in the validation cohorts. In the Survival Validation Cohort, Group 1 had better survival than Group 2 (HR 0.49 [0.37–0.65], p<0.001). In the Echo Validation Cohort, Group 1 had better LVEF response than Group 2 (mean LVEF change 9.8±10.0% vs. 5.5±7.9%, p=0.025). Patient characteristics and full subgroup comparisons in each of the cohorts are provided in Supplemental Tables 1–6. Lead subset analysis compared to 12-lead analysis did not improve primary outcome stratification (Supplemental Table 7). Clusters were robust to different methods of validation (Supplemental Table 8).

Overall, QRS PCA Group 1 contained 521 patients (456 LBBB, 0 RBBB, 65 IVCD). QRS PCA Group 2 contained 425 patients (142 LBBB, 119 RBBB, 164 IVCD). Group 1 had more LBBB, longer QRSd, higher proportion of females and non-ischemic cardiomyopathy, lower proportion of atrial fibrillation, and better renal function (Table 1). Full subgroup comparisons of primary outcomes are provided in Table 2. Full subgroup comparisons of CRT response (LVEF change ≥5%) and super-response (LVEF change ≥20%) rates are provided in Supplemental Table 9. QRS PCA Group 1 had better event-free survival and greater LVEF improvement than Group 2 (HR 0.44, 95% CI [0.38–0.53], p<0.001; mean LVEF change 11.1±11.7% vs. 4.8±9.7%, p<0.001; Figure 3), and had higher CRT response (69% vs 50%, p<0.001) and super-response rates (26% vs 9%, p<0.001). Among LBBB and QRSd ≥150 ms patients, QRS PCA Group 1 still had reduced risk for the composite endpoint and greater overall LVEF response (HR 0.42, 95% CI [0.33–0.55], p<0.001; mean LVEF change 12.5±11.8% vs. 7.3±8.1%, p=0.002; Figure 3), but exhibited similar CRT response rates (74% vs. 66%, p=0.23) with higher super-response rates (29% vs. 8%, p<0.001). QRS PCA Groups did not stratify outcomes within non-LBBB patients (HR 0.79,

95% CI [0.57–1.12], p=0.18; mean LVEF change 2.0±8.4% vs. 3.8±10.1%, p=0.32). Group 1 had greater reduction in secondary outcomes: LVEDD, LVESD, MR grade, and NYHA status (Supplemental Table 10).

Nonlinear dimensionality reduction discriminated outcomes similarly to PCA (Supplemental Table 11). Using k=3 or k=4 clusters identified groups showed that higher PCA scores conferred better outcomes (Supplemental Figure 3). Including or excluding QRSd and QRS area with the 12-lead QRS waveforms during the PCA and clustering process resulted in similar cluster identification and outcome discrimination (Supplemental Table 12).

Multivariable models for primary outcomes included age, male sex, ischemic cardiomyopathy, QRSd, LBBB, history of atrial fibrillation, creatinine, presence of end-stage renal disease on hemodialysis, and QRS PCA group (Supplemental Table 13). In multivariable Cox regression for the composite endpoint, age, male sex, ischemic cardiomyopathy, atrial fibrillation, high creatinine, hemodialysis, QRSd <150 ms, and QRS PCA group 2 were significantly associated with mortality. QRS PCA group was not an independent predictor in multivariable linear regression for LVEF change, while male sex, ischemic cardiomyopathy, non-LBBB, and QRSd <150 ms were. QRS area was significantly correlated with the QRS PCA score (r=0.75, p<0.001), and QRS area groups exhibited comparable outcome differentiation compared to QRS PCA groups (Table 2). However, QRS PCA groups had significantly different outcomes within QRS area groups, and vice versa.

A supervised classifier incorporating QRSd, QRS morphology, QRS area, and QRS PCA representation had higher prediction performance metrics than any ECG characteristics alone, but did not improve echocardiographic CRT response prediction from the QRS PCA representation alone (Supplemental Table 14). Adding QRS PCA representation and QRS area a supervised machine learning classifier trained by 9 common clinical variables[25] to predict echocardiographic CRT response did not improve LVEF response prediction, but slightly improved discriminating long-term survival (Supplemental Table 14).

572 patients had LV lead location recorded, distributed along the long axis with 159 (28%) apical, 347 (61%) midventricular, and 66 (12%) basal, and distributed along the short axis with 22 (4%) anterior, 167 (29%), and 383 (67%) posterior. Apical LV lead location was associated with an increased risk for the composite endpoint (HR 1.31, 95% CI [1.01–1.69], p=0.039), but no other lead locations had differing long-term outcomes or LVEF change. Within QRS PCA Group 1, midventricular LV lead location was associated with greater LVEF improvement than non-midventricular leads (13.1% vs. 9.8%, p=0.042), but would not remain significant after correcting for multiple comparisons. No other interactions with QRS PCA groups were observed (Supplemental Figure 4).

Stratifying QRS morphology by QRS PCA group and QRS area

In subgroups defined by QRS morphology and QRSd, patients with non-LBBB and QRSd<150 ms had the worst survival (5-year survival rate 0.48, Figure 4A) and lowest LVEF change (2.5±9.5%). Non-LBBB patients with QRSd≥150 ms, LBBB patients with

QRSd <150 ms, then LBBB patients with QRSd ≥150 ms had incrementally better outcomes (Figure 4A).

When stratifying conduction morphology by QRS PCA group and QRS area, patients with non-LBBB, QRS area ≤95 μVs, and QRS PCA Group 2 had a 5-year event-free survival rate of 0.48 (Figure 4B) and a mean LVEF change of 3.6±10.2%. Non-LBBB patients with QRS area >95 μVs or QRS PCA Group 1 had slightly improved survival but not better LVEF improvement, and LBBB patients with QRS area >95 μVs or QRS PCA Group 1 had substantially improved survival and LVEF improvement (Figure 4B). LBBB patients with QRS area ≤95 μVs and QRS PCA Group 2 had similar outcomes compared to patients with non-LBBB (HR 1.32, 95% CI [0.93–1.62]; mean LVEF change 4.34±7.9% vs. 3.5±9.8%, 95% CI for difference: [−2.1% to 3.7%]).

There were 18.5% more LBBB patients with QRS area >95 μVs or QRS PCA Group 1 (n=513) than LBBB patients with QRSd ≥150 ms (n=433), representing an expansion from Class I ECG criteria. Only 36 (8%) of LBBB patients with QRSd ≥150 ms had QRS area ≤95 μVs and QRS PCA Group 2 assignment. 116 (70%) LBBB patients with QRSd <150 ms had QRS area >95 μVs or QRS PCA Group 1 assignment. Despite lacking a Class I CRT indication, these patients had comparable survival (HR: 0.93, 95% CI: [0.67–1.29]) and LVEF improvement (mean 11.3±11.1% vs. 11.5±11.4%, 95% CI for difference: [−2.7% to 3.0%]) to LBBB patients with QRSd ≥150 ms. Reclassification results are provided in Supplemental Table 15. Figure 5 compares selection of LBBB patients using QRSd versus QRS area and QRS PCA groups.

Discussion

We sought to use machine learning of QRS waveforms to enhance CRT patient selection beyond traditional ECG markers. Using principal components analysis (PCA) to represent 12-lead QRS patterns in two dimensions and *k*-means clustering, we identified two groups with higher and lower long-term survival and echocardiographic improvement, even among patients with Class I ECG criteria (LBBB, QRSd ≥150 ms) who would be expected to have better outcomes. Stratifying LBBB by QRS area and QRS PCA representation identified LBBB patients with QRSd <150 ms who had similar outcomes to LBBB patients with QRSd ≥150 ms, and also identified LBBB patients with outcomes similar to non-LBBB patients. Such methods may yield more objective mechanisms of patient selection than subjective LBBB labeling.

Machine learning is being increasingly explored to interrogate complex ECG patterns. Deep learning of ECGs has classified arrhythmia[26] and screened for LV dysfunction[27] and hyperkalemia[28]. Unsupervised machine learning of ECG morphology identified phenotypes of hypertrophic cardiomyopathy[29]. In CRT, machine learning has been used to predict CRT response from common clinical variables[25,30] and identify CRT responders from complex echocardiogram traces and clinical data[20].

To our knowledge, this study was the first machine learning analysis of ECG waveforms to identify meaningful CRT patient subgroups. The approach was different from traditional

ECG analysis because we compositely evaluated 12-lead waveforms instead of using computed metrics on a per-lead basis. The approach was distinct from many machine learning approaches because it avoided a “black box” model; the PCA dimensionality reduction transformation can be directly replicated on external data (unlike many other non-linear dimensionality reduction algorithms) and is interpretable via the mapping vector. The validation experiment in this study served as a proof-of-concept in how one might apply the PCA transformation identified in this study to external digitized ECG data. Similar methodology could be used for ECG or other digital waveform analysis in other cardiovascular investigations.

It is important to note that other clinical variables that are known predictors of reduced CRT response were represented with higher proportion in QRS PCA group 2 (non-LBBB, narrower QRSd, male gender, ischemic disease, history of AF). However, in multivariable adjustment and basic supervised machine learning experiments, adding QRS PCA groups to clinical variables did enhance mortality prediction, but did not enhance prediction of LVEF response (Supplemental Tables 13–14). Therefore, it is unclear if the advantage of the ECG tool developed in this study goes beyond solely using the ECG to capture other biological predictors of CRT response.

Though the PCA mapping vector does not provide the precise physiological underpinnings of the different QRS PCA groups, it affirmed the importance of LBBB, and also suggested why some LBBB patients received a low QRS PCA score (Figure 2): lower voltage amplitudes, and negative deflection in leads II, aVF, V5, and V6. Low amplitude may be associated with ischemic disease and reduced myocardial viability[15,16,31]. Concordantly, QRS PCA Group 2 had a higher proportion of ischemic cardiomyopathy. Interestingly, the QRS PCA score was well-correlated with vectorcardiographic QRS area, another predictive ECG biomarker for CRT outcomes[15,16,23], and the QRS PCA mapping vector was similar to the Kors transform from 12-lead ECG to the vectorcardiographic Z-axis[32] (Supplemental Figure 5). This suggests that the Z-axis of QRS area reflects the primary component of variance in QRS patterns of conduction delay, affirming the importance of the Z-axis in LBBB and CRT[11,33,34]. Despite similarities between QRS area and the QRS PCA representation, there also existed significant differences, possibly due to the X- and Y-components of QRS area.

QRS PCA group and QRS area effectively stratified LBBB, more so than QRSd. While this study lacks a non-CRT control group to assess CRT benefit, the study may be useful in objectively affirming which LBBB patients (with or without a wide QRS) are likely to have better long-term survival and echocardiographic improvement following CRT (Figure 5). Stratifying LBBB by QRS PCA and QRS area groups identified LBBB patients with QRSd <150 ms who had similar outcomes to LBBB patients with QRSd ≥150 ms. Conversely, LBBB patients that were stratified as unfavorable by QRS PCA group and QRS area had similar survival and LVEF outcomes to non-LBBB patients. This work may facilitate future studies seeking to refine CRT guidelines or identify heart failure patients who may better benefit from alternative emerging device-based therapies[35–37].

Limitations

This study was single-center and retrospective, and validation cohorts were internal, significantly biasing the generalizability of the results. Analysis did not assess CRT outcomes compared to a non-CRT control group. We did not study right ventricular-paced or narrow QRS patients. QRS area nor QRS PCA group significantly stratified LVEF change in subgroups of the Echo Validation Cohort. There are several potential explanations. Sample size was limited (60 LBBB patients with QRSd ≥150 ms) and echo follow-up time was shorter than in the Primary Cohort (6.6 versus 9.1 months). The Echo Validation Cohort was more contemporary, which may reflect changing procedural techniques.

The QRS PCA representation was empirically derived, and thus dependent on the patient population. However, the QRS PCA representation was robust (Supplemental Figure 2), agreed with the QRS area Z-axis, and was evaluated independently on multiple cohorts. The QRS PCA representation is objective, interpretable, and can be calculated on new data. Practical use would require digitized ECGs, but could be implemented and reported with routine preliminary ECG interpretations available today.

Conclusions

12-lead ECG analysis using PCA and *k*-means clustering of QRS waveforms identified CRT groups with differential outcomes, even among LBBB patients with QRSd ≥150 ms. QRS area was validated as an ECG biomarker for CRT response. Stratification of LBBB by QRS area and QRS PCA representation identified patients without Class I ECG indications who had equally favorable outcomes, and LBBB patients who had poorer outcomes similar to non-LBBB patients. This stratification of LBBB may represent an objective mechanism for CRT patient selection without requiring subjective strict LBBB definition. Our study presents compelling data for 12-lead ECG waveform dimensionality reduction and unsupervised clustering to identify and interpret meaningful patient subgroups.

Supplementary Material

Refer to Web version on PubMed Central for supplementary material.

Acknowledgments

Sources of Funding: The study was supported by NIH/NHLBI R01-HL111314, American Heart Association Atrial Fibrillation Strategically Focused Research Network grant, NIH UL1-RR024989, Center of Excellence in Cardiovascular Translational Functional Genomics, Heart & Vascular Institute and Lerner Research Institute and Philanthropy funds, Tomsich Atrial Fibrillation Research Fund, NCI/NIH: 1U24CA199374-01, R01CA202752-01A1, R01CA208236-01A1, R01-CA216579-;01A1, R01-CA220581-01A1, 1U01-CA239055-01, National Center for Research Resources 1-C06 RR12463-01, Veterans Affairs Award IBX004121A, Department of Defense Awards: W81XWH-15-1-0558, W81XWH-18-1-0440, W81XWH-16-1-0329, Ohio Third Frontier Technology Validation Fund, Wallace H. Coulter Foundation Program in the Department of Biomedical Engineering, and the Clinical and Translational Science Award Program at Case Western Reserve University. The content is solely the responsibility of the authors and does not necessarily represent official views of the NIH, Veterans Affairs, Department of Defense, or US Government.

Nonstandard Abbreviations and Acronyms

CRT	cardiac resynchronization therapy

QRSd	QRS duration
LBBB	left bundle branch block
LV	left ventricular
PCA	principal components analysis
LVEF	left ventricular ejection fraction
RBBB	right bundle branch block
IVCD	non-specific intraventricular conduction delay
LVAD	left ventricular assist device
LVEDD	left ventricular end-diastolic diameter
LVESD	left ventricular end-systolic diameter
MR	mitral regurgitation
NYHA	New York Heart Association

References:

1. Bristow MR, Saxon LA, Boehmer J, Krueger S, Kass DA, DeMarco T, Carson P, DiCarlo L, DeMets D, White BG, et al. Cardiac-Resynchronization Therapy with or without an Implantable Defibrillator in Advanced Chronic Heart Failure. New Engl J Med. 2004;350,2140–2150. [PubMed: 15152059]
2. Tang ASL, Wells GA, Talajic M, Arnold MO, Sheldon R, Connolly S, Hohnloser SH, Nichol G, Birnie DH, Sapp JL, et al. Cardiac-Resynchronization Therapy for Mild-to-Moderate Heart Failure. New Engl J Med. 2010;363,2385–2395. [PubMed: 21073365]
3. Cleland JGF, Daubert J-C, Erdmann E, Freemantle N, Gras D, Kappenberger L, Tavazzi L. The Effect of Cardiac Resynchronization on Morbidity and Mortality in Heart Failure. New Engl J Med. 2005;352,1539–1549. [PubMed: 15753115]
4. Vernooy K, van Deursen CJM, Strik M, Prinzen FW. Strategies to improve cardiac resynchronization therapy. Nat Rev Cardiol. 2014;11,481–493. [PubMed: 24839977]
5. Yancy CW, Jessup M, Bozkurt B, Butler J, Casey DE, Drazner MH, Fonarow GC, Geraci SA, Horwich T, Januzzi JL, et al. 2013 ACCF/AHA Guideline for the Management of Heart Failure: A Report of the American College of Cardiology Foundation/American Heart Association Task Force on Practice Guidelines. Circulation. 2013;CIR.0b013e31829e8776.
6. Varma N Left Ventricular Conduction Delays and Relation to QRS Configuration in Patients With Left Ventricular Dysfunction. Am J Cardiol. 2009;103,1578–1585. [PubMed: 19463519]
7. Zweerink A, Friedman DJ, Klem I, van de Ven PM, Vink C, Biesbroek PS, Hansen SM, Emerek K, Kim RJ, van Rossum AC, et al. Size Matters: Normalization of QRS Duration to Left Ventricular Dimension Improves Prediction of Long-Term Cardiac Resynchronization Therapy Outcome. Circ Arrhythm Electrophysiol. 2018;11,e006767. [PubMed: 30541355]
8. Dupont M, Rickard J, Baranowski B, Varma N, Dresing T, Gabi A, Finucan M, Mullens W, Wilkoff BL, Tang WHW. Differential Response to Cardiac Resynchronization Therapy and Clinical Outcomes According to QRS Morphology and QRS Duration. J Am Coll Cardiol. 2012;60,592–598. [PubMed: 22796255]
9. Strauss DG, Selvester RH, Wagner GS. Defining Left Bundle Branch Block in the Era of Cardiac Resynchronization Therapy. Am J Cardiol. 2011;107,927–934. [PubMed: 21376930]

10. van Stipdonk AMW, Vanbelle S, Ter Horst IH, Luermans JG, Meine M, Maass AH, Auricchio A, Prinzen FW, Vernooy K. Large variability in clinical judgement and definitions of left bundle branch block to identify candidates for cardiac resynchronisation therapy. Int J Cardiol. 2019;286,61–65. [PubMed: 30661850]
11. Niebauer MJ, Rickard J, Polakof L, Tchou PJ, Varma N. QRS frequency characteristics help predict response to cardiac resynchronization in left bundle branch block less than 150 milliseconds. Heart Rhythm. 2014;11,2183–2189. [PubMed: 25068573]
12. Del-Carpio Munoz F, Powell BD, Cha YM, Wiste HJ, Redfield MM, Friedman PA, Asirvatham SJ. Delayed intrinsicoid deflection onset in surface ECG lateral leads predicts left ventricular reverse remodeling after cardiac resynchronization therapy. Heart Rhythm. 2013;10,979–987. [PubMed: 23542361]
13. Eitel C, Wilton SB, Switzer N, Cowan K, Exner DV. Baseline delayed left ventricular activation predicts long-term clinical outcome in cardiac resynchronization therapy recipients. Europace. 2012;14,358–364. [PubMed: 21933803]
14. Tereshchenko LG, Cheng A, Park J, Wold N, Meyer TE, Gold MR, Mittal S, Singh J, Stein KM, Ellenbogen KA. Novel measure of electrical dyssynchrony predicts response in cardiac resynchronization therapy: Results from the SMART-AV Trial. Heart Rhythm. 2015;12,2402–2410. [PubMed: 26272523]
15. van Deursen CJM, Vernooy K, Dudink E, Bergfeldt L, Crijns HJGM, Prinzen FW, Wecke L Vectorcardiographic QRS area as a novel predictor of response to cardiac resynchronization therapy. J Electrocardiol. 2015;48,45–52. [PubMed: 25453196]
16. Emerek K, Friedman DJ, Sørensen PL, Hansen SM, Larsen JM, Risum N, Thøgersen AM, Graff C, Kisslo J, Søgaard P, Atwater BD. Vectorcardiographic QRS area is associated with long-term outcome after cardiac resynchronization therapy. Heart Rhythm. 2018;10.1016/j.hrthm.2018.08.028.
17. Lambiase PD. Defining left bundle branch block-Is this a roadblock to CRT delivery? Int J Cardiol. 2019;286,78–80. [PubMed: 30928259]
18. Tiwari P, Rosen M, Madabhushi A. A hierarchical spectral clustering and nonlinear dimensionality reduction scheme for detection of prostate cancer from magnetic resonance spectroscopy. Medical Physics. 2009;36,3927–3939. [PubMed: 19810465]
19. Tiwari P, Rosen M, Reed G, Kurhanewicz J, Madabhushi A. Spectral Embedding Based Probabilistic Boosting Tree: Classifying High Dimensional Heterogeneous Biomedical Data. MICCAI 2009 844–851. [PubMed: 20426190]
20. Cikes M, Sanchez-Martinez S, Claggett B, Duchateau N, Piella G, Butakoff C, Pouleur AC, Knappe D, Biering-Sørensen T, Kutyifa V, et al. Machine learning-based phenogrouping in heart failure to identify responders to cardiac resynchronization therapy. Eur J Heart Fail. 2019;21,74–85. [PubMed: 30328654]
21. Gorodeski EZ, Magnelli-Reyes C, Moennich LA, Grimaldi A, Rickard J. Cardiac resynchronization therapy-heart failure (CRT-HF) clinic: A novel model of care. PLOS ONE. 2019;14,e0222610. [PubMed: 31536565]
22. Waks JW, Sitlani CM, Soliman EZ, Kabir M, Ghafoori E, Biggs ML, Henrikson CA, Sotoodehnia N, Biering-Sørensen T, Agarwal SK, et al. Global Electrical Heterogeneity Risk Score for Prediction of Sudden Cardiac Death in the General Population: The Atherosclerosis Risk in Communities (ARIC) and Cardiovascular Health (CHS) Studies. Circulation. 2016;133,2222–2234. [PubMed: 27081116]
23. van Stipdonk AMW, ter Horst I, Kloosterman M, Engels EB, Rienstra M, Crijns HJGM, Vos Marc A, van Gelder IC, Prinzen FW, Meine M, et al. QRS Area Is a Strong Determinant of Outcome in Cardiac Resynchronization Therapy. Circ Arrhythm Electrophysiol. 2018;11,e006497. [PubMed: 30541356]
24. Emerek K, Friedman DJ, Sørensen PL, Hansen SM, Larsen JM, Risum N, Thøgersen AM, Graff C, Kisslo J, Søgaard P, Atwater BD. Vectorcardiographic QRS area is associated with long-term outcome after cardiac resynchronization therapy. Heart Rhythm. 2019;16,213–219. [PubMed: 30170227]

25. Feeny AK, Rickard J, Patel D, Toro S, Trulock KM, Park CJ, LaBarbera MA, Varma N, Niebauer MJ, Sinha S, et al. Machine Learning Prediction of Response to Cardiac Resynchronization Therapy. Circ Arrhythm Electrophysiol. 2019;12,e007316. [PubMed: 31216884]
26. Hannun AY, Rajpurkar P, Haghpanahi M, Tison GH, Bourn C, Turakhia MP, Ng AY. Cardiologist-level arrhythmia detection and classification in ambulatory electrocardiograms using a deep neural network. Nat Med. 2019;25,65. [PubMed: 30617320]
27. Attia ZI, Kapa S, Lopez-Jimenez F, McKie PM, Ladewig DJ, Satam G, Pellikka PA, Enriquez-Sarano M, Noseworthy PA, Munger TM, et al. Screening for cardiac contractile dysfunction using an artificial intelligence-enabled electrocardiogram. Nat Med. 2019;25,70. [PubMed: 30617318]
28. Galloway CD, Valys AV, Shreibati JB, Treiman DL, Petterson FL, Gundotra VP, Albert DE, Attia ZI, Carter RE, Asirvatham SJ, et al. Development and Validation of a Deep-Learning Model to Screen for Hyperkalemia From the Electrocardiogram. JAMA Cardiol. 2019;10.1001/jamacardio.2019.0640.
29. Lyon A, Ariga R, Mincholé A, Mahmod M, Ormondroyd E, Laguna P, de Freitas N, Neubauer S, Watkins H, Rodriguez B. Distinct ECG Phenotypes Identified in Hypertrophic Cardiomyopathy Using Machine Learning Associate With Arrhythmic Risk Markers. Front Physiol. 2018;9,213. [PubMed: 29593570]
30. Kalscheur MM, Kipp RT, Tattersall MC, Mei C, Buhr KA, DeMets DL, Field ME, Eckhardt LL, Page CD. Machine Learning Algorithm Predicts Cardiac Resynchronization Therapy Outcomes: Lessons From the COMPANION Trial. Circ Arrhythm Electrophysiol. 2018;11,e005499. [PubMed: 29326129]
31. Nguyên UC, Claridge S, Vernooy K, Engels EB, Razavi R, Rinaldi CA, Chen Z, Prinzen FW. Relationship between vectorcardiographic QRSarea, myocardial scar quantification, and response to cardiac resynchronization therapy. J Electrocardiol. 2018;51,457–463. [PubMed: 29454649]
32. Vozda M, Cerny M. Methods for derivation of orthogonal leads from 12-lead electrocardiogram: A review. Biomedical Signal Processing and Control. 2015;23–34.
33. Wallace AG, Ester EH, McCall BW. The vectorcardiographic findings in left bundle branch block: A study using the Frank lead system. American Heart Journal 1962;63,508–515 [PubMed: 14004644]
34. DE Pooter J, El Haddad M, DE Buyzere M, Aranda HA, Cornelussen R, Stegemann B, Rinaldi CA, Sterlinski M, Sokal A, Francis DP, et al. Biventricular Paced QRS Area Predicts Acute Hemodynamic CRT Response Better Than QRS Duration or QRS Amplitudes. J Cardiovasc Electrophysiol. 2017;28,192–200. [PubMed: 27885752]
35. Reddy VY, Miller MA, Neuzil P, Søgaard P, Butter C, Seifert M, Delnoy PP, van Erven L, Schalji M, Boersma LVA, Riahi S. Cardiac Resynchronization Therapy With Wireless Left Ventricular Endocardial Pacing: The SELECT-LV Study. J Am Coll Cardiol. 2017;69,2119–2129. [PubMed: 28449772]
36. Smith S, Rossignol P, Willis S, Zannad F, Mentz R, Pocock S, Bisognano J, Nadim Y, Geller N, Ruble S, Linde C. Neural modulation for hypertension and heart failure. Int J Cardiol. 2016;214,320–330. [PubMed: 27085120]
37. Abraham WT, Kuck K-H, Goldsmith RL, Lindenfeld J, Reddy VY, Carson PE, Mann DL, Saville B, Parise H, Chan R, et al. A Randomized Controlled Trial to Evaluate the Safety and Efficacy of Cardiac Contractility Modulation. J Am Coll Cardiol HF. 2018;6,874–883.

What is Known

- Left bundle branch block (LBBB) and QRS duration are the primary ECG characteristics used for CRT patient selection
- LBBB is the strongest ECG predictor for positive CRT response, but has unstandardized definitions and requires subjective assessment

What the Study Adds

- Unsupervised ML of baseline QRS waveforms was used to identify 2 groups of CRT patients with differential outcomes, even among patients with LBBB and QRS duration >150 ms
- For CRT patient selection, this methodology was useful in objective identification of which subjectively labeled LBBB patients were strong CRT candidates, and which had outcomes more similar to non-LBBB patients

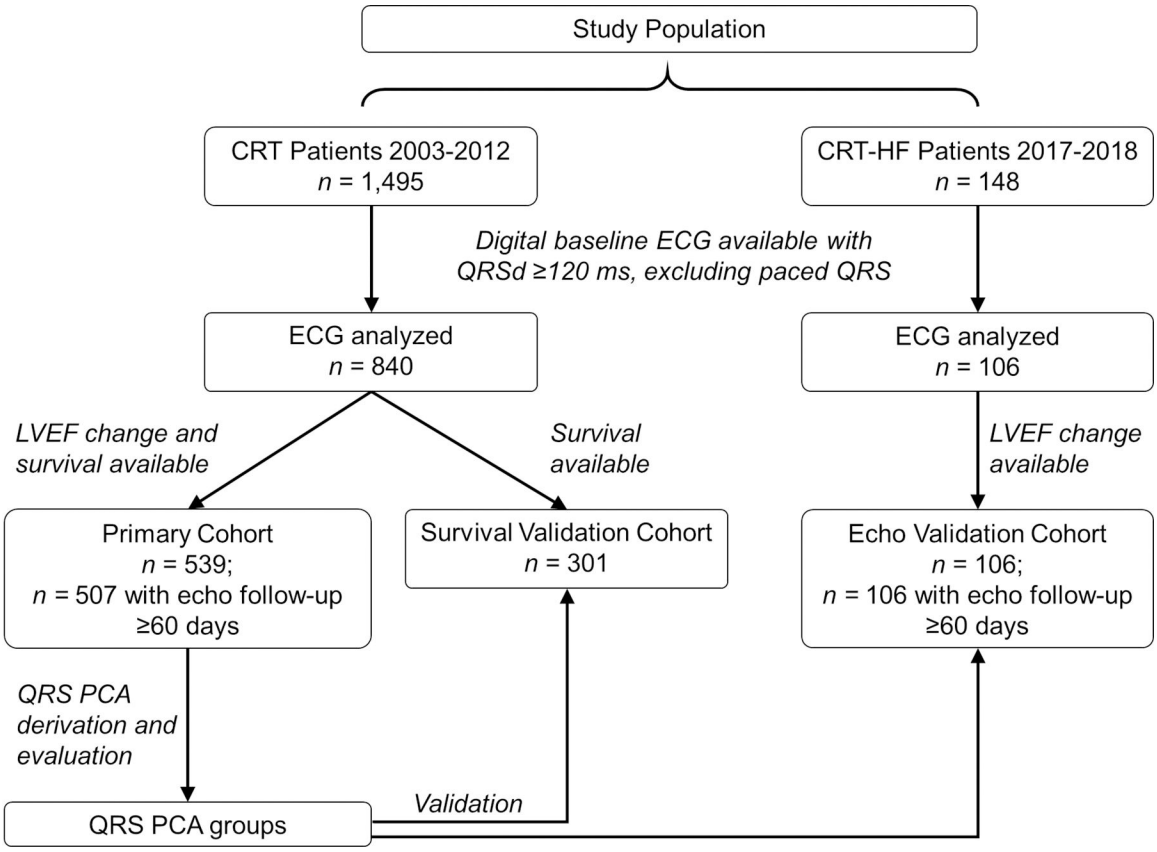

Figure 1:

Study population and design. CRT=cardiac resynchronization therapy. CRT-HF=CRT heart failure clinic. QRSd=QRS duration. LVEF=left ventricular ejection fraction. PCA=principal components analysis.

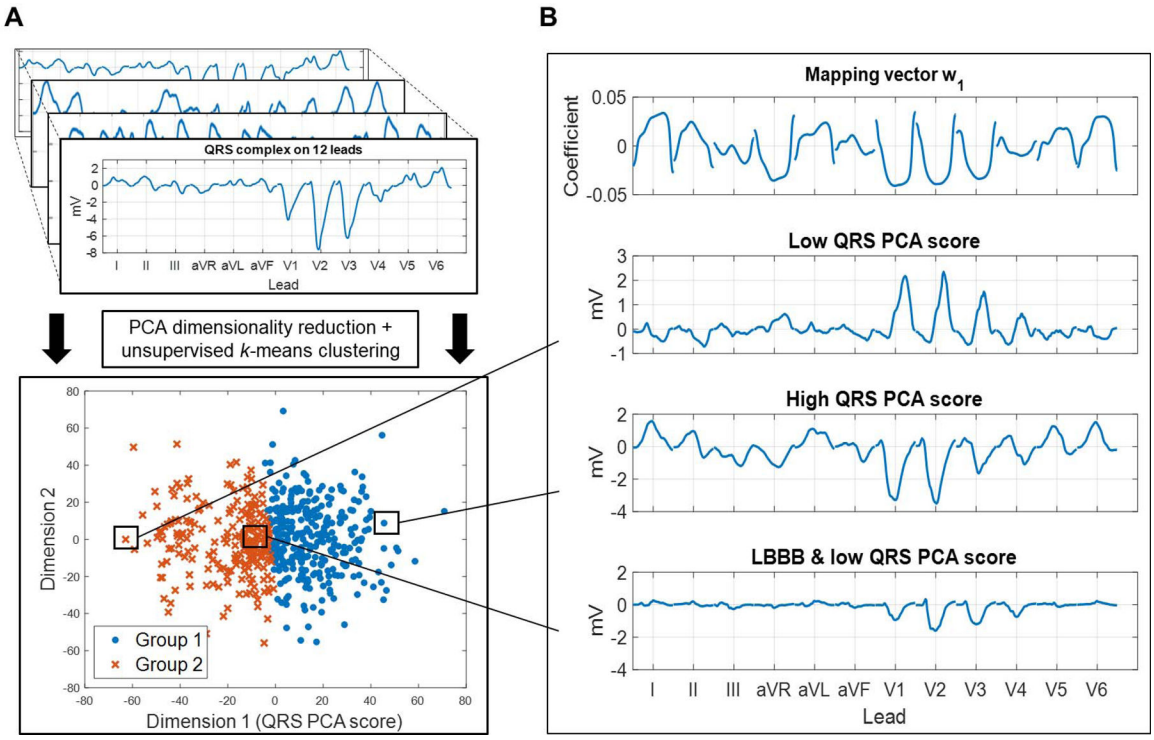

Figure 2:

(A) Overview of the unsupervised machine learning. Feature vectors containing 12-lead QRS patterns were extracted from 539 cardiac resynchronization therapy (CRT) patients in the Primary Cohort, and were used as input to a pipeline using principal components analysis (PCA) dimensionality reduction followed by *k*-means clustering to identify two groups. **(B)** From top: (1) Mapping vector $\mathbf{w_1}$ determined the QRS PCA score via the dot product of $\mathbf{w_1}$ and the standardized QRS feature vector (Supplemental Methods Equation 1). (2) Feature vector* with a low QRS PCA score and right bundle branch block. (3) Feature vector* with a high QRS PCA score, driven by a left bundle branch block (LBBB) pattern with marked positive deflections in leads I, II, aVL, V5, and V6. (4) Feature vector* with low QRS PCA score despite LBBB. Lower voltage amplitudes drive the low QRS PCA score. *Before standardization.

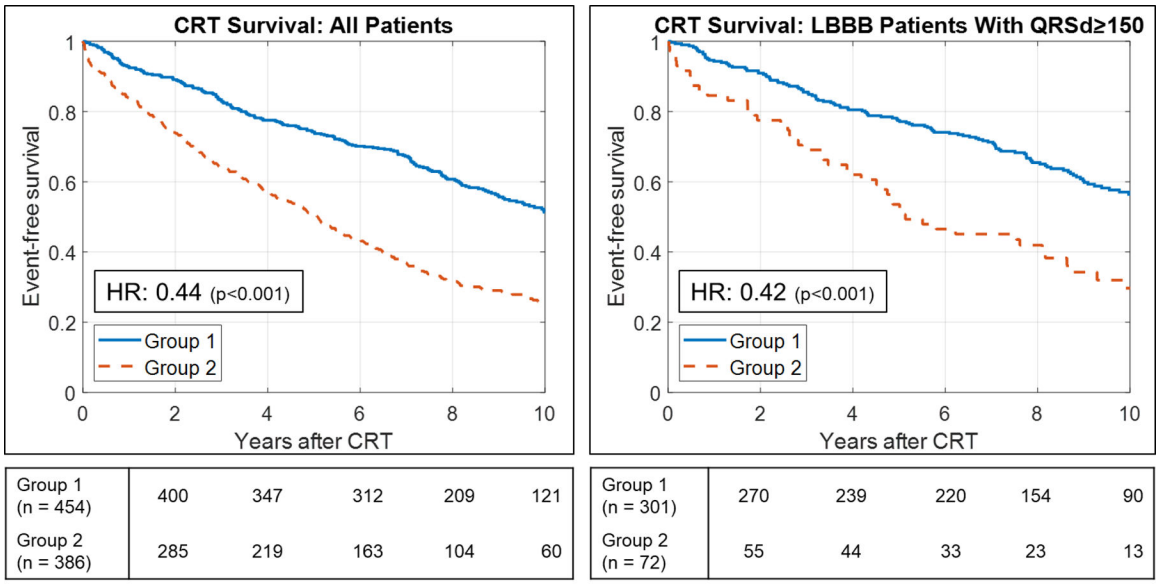

Group 1 (n = 454)	400	347	312	209	121
Group 2 (n = 386)	285	219	163	104	60

Group 1 (n = 301)	270	239	220	154	90
Group 2 (n = 72)	55	44	33	23	13

Figure 3:

Survival after cardiac resynchronization therapy (CRT) in groups identified by principal components analysis (PCA) of 12-lead QRS waveforms followed by k-means clustering. Kaplan-Meier curves depicting event-free survival from death, left ventricular assist device, or heart transplant after CRT implant with univariable hazard ratios (HR).

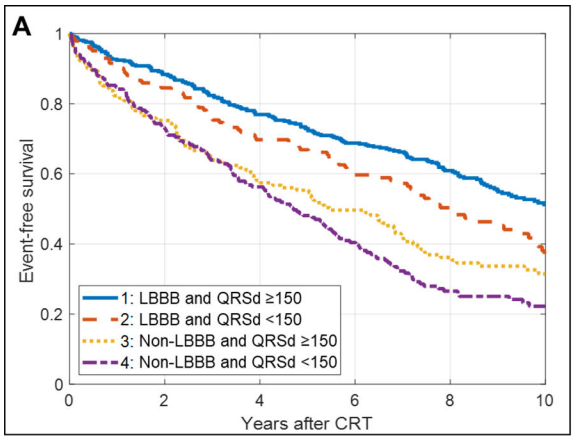

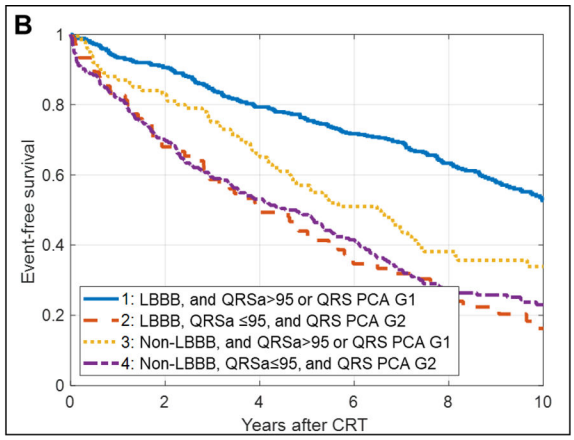

Group	Number at Risk				
1 (n = 373)	325	283	253	177	103
2 (n = 143)	120	98	83	52	30
3 (n = 141)	106	82	67	47	28
4 (n = 183)	134	103	72	37	20

Cox Proportional Hazards (Reference: Group 4)	Hazard Ratio (95% CI)	p
Group 1	0.45 (0.36 – 0.56)	<0.001
Group 2	0.58 (0.44 – 0.76)	<0.001
Group 3	0.86 (0.67 – 1.11)	0.25

	LVEF Change (%)	P (versus Group 4)
Group 1	11.5 ± 11.4	<0.001
Group 2	9.0 ± 10.9	<0.001
Group 3	5.0 ± 10.1	0.079
Group 4	2.5 ± 9.5	n/a

LVEF Responder Rates	Worseners (LVEF change <0%)	Responders (LVEF change ≥5%)	Super-responders (LVEF change ≥20%)
Group 1	10%	72%	25%
Group 2	16%	64%	20%
Group 3	16%	43%	11%
Group 4	32%	43%	5%

Group	Number at Risk				
1 (n = 441)	394	344	310	212	125
2 (n = 75)	51	37	26	17	8
3 (n = 100)	83	66	50	32	17
4 (n = 224)	157	119	89	52	31

Cox Proportional Hazards (Reference: Group 4)	Hazard Ratio (95% CI)	p
Group 1	0.40 (0.33 – 0.49)	<0.001
Group 2	1.12 (0.84 – 1.49)	0.45
Group 3	0.74 (0.56 – 0.98)	0.038

	LVEF Change (%)	P (versus Group 4)
Group 1	11.7 ± 11.4	<0.001
Group 2	4.3 ± 7.9	0.63
Group 3	3.4 ± 8.7	0.90
Group 4	3.6 ± 10.2	n/a

LVEF Responder Rates	Worseners (LVEF change <0%)	Responders (LVEF change ≥5%)	Super-responders (LVEF change ≥20%)
Group 1	10%	72%	27%
Group 2	23%	54%	2%
Group 3	24%	40%	5%
Group 4	26%	45%	8%

Figure 4:

Survival after cardiac resynchronization therapy (CRT) stratified by ECG characteristics. Kaplan-Meier curves depict event-free survival from death, left ventricular assist device, or heart transplant after CRT implant, with univariable hazard ratios (HR). **A.** Stratification by conduction morphology and QRS duration (QRSd). **B.** Stratification by conduction morphology, QRS area (QRSa), and QRS principal components analysis Group 1 (QRS PCA G1) versus Group 2 (QRS PCA G2). LBBB=left bundle branch block. LVEF=left ventricular ejection fraction. QRSd units in ms. QRSa units in μVs.

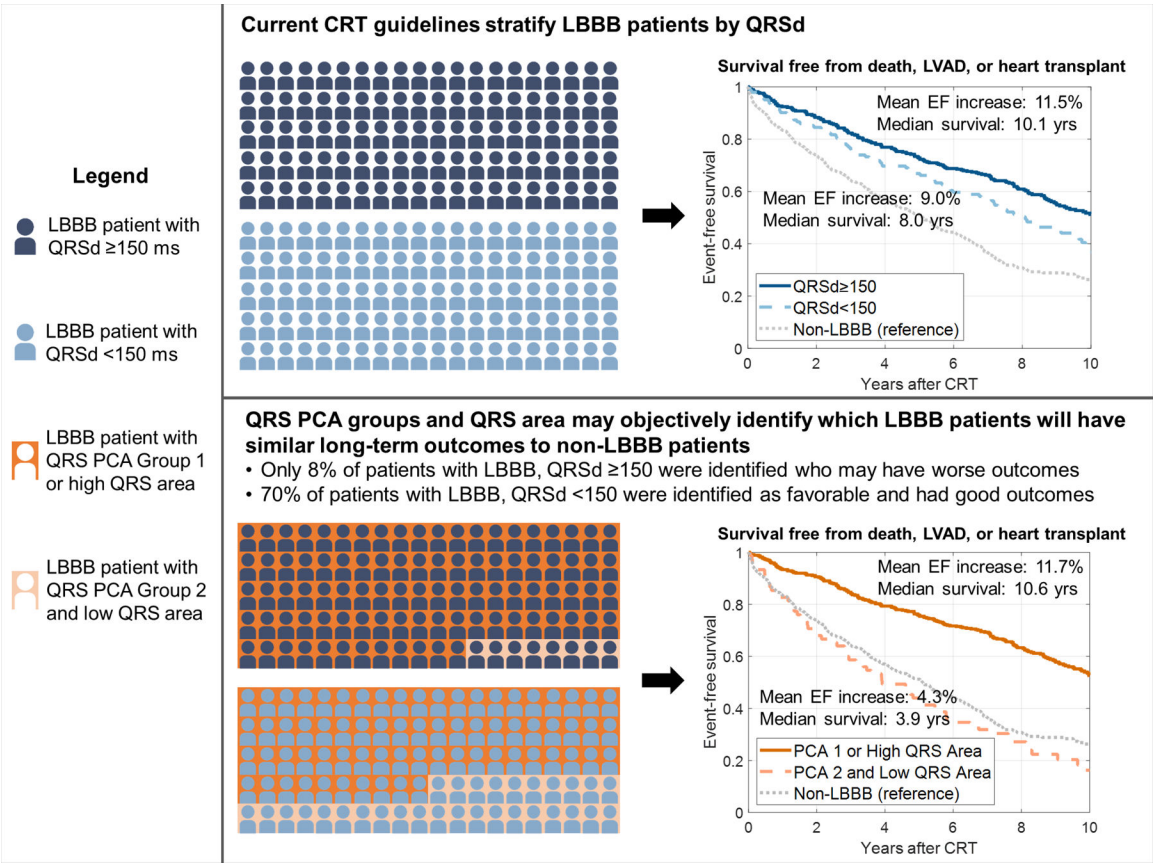

Figure 5:

Comparison of left bundle branch block (LBBB) cardiac resynchronization therapy (CRT) patient selection using QRS duration (QRSd) versus QRS principal components analysis (PCA) and QRS area. LVAD=left ventricular assist device. EF=ejection fraction. High vs. low QRS area was defined by a cutoff of 95 μVs.

Table 1.

Baseline characteristics

	Entire cohort (*n*=946)	QRS PCA Group 1 (*n*=521)	QRS PCA Group 2 (*n*=425)	p
Demographics and medical history				
Age (years)	66.5±11.8	65.81±11.9	67.4±11.6	0.035
Male sex	628 (66.7%)	301 (58.1%)	327 (77.1%)	<0.001
Body mass index (kg/m^2)	28.9±6.4	28.9±6.5	28.8±6.4	0.69
Ischemic cardiomyopathy	470 (56.0%)	202 (44.5%)	268 (69.4%)	<0.001
NYHA functional class				0.27
I	11 (1.2%)	8 (1.5%)	3 (0.8%)	
II	87 (10.4%)	54 (11.9%)	33 (8.5%)	
III	701 (83.5%)	378 (83.3%)	323 (83.7%)	
IV	41 (4.9%)	14 (3.1%)	27 (7.0%)	
History of atrial fibrillation	401 (47.7%)	192 (42.3%)	209 (54.1%)	0.001
Hypertension	532 (63.3%)	298 (65.6%)	234 (60.6%)	0.15
Tobacco use	494 (59.7%)	263 (58.7%)	231 (60.8%)	0.59
Hyperlipidemia	502 (59.8%)	259 (57.0%)	243 (63.0%)	0.095
Chronic obstructive pulmonary disease	116 (13.8%)	64 (14.1%)	52 (13.5%)	0.87
Cerebrovascular accident or transient ischemic attack	91 (10.8%)	44 (9.7%)	47 (12.2%)	0.30
History of malignancy	100 (11.9%)	54 (11.9%)	46 (11.9%)	>0.99
End-stage renal disease on hemodialysis	23 (2.7%)	7 (1.5%)	16 (4.1%)	0.036
Diabetes mellitus	322 (38.3%)	175 (38.5%)	147 (38.1%)	0.95
Echocardiography				
LVEF (%)	23.5±8.8	23.5±8.6	23.6±9.2	0.80
LVEDD (cm)	6.1±1.0	6.0±1.1	6.1±0.9	0.43
LVESD (cm)	5.1±1.3	5.2±1.5	5.1±1.0	0.70
Mitral regurgitation grade (1–9)	3.0 [1.0,5.0]	3.0 [1.0,5.0]	4.0 [2.0,5.0]	0.22
Electrocardiography				
QRS duration (ms)	156.0±20.4	159.8±20.4	151.5±19.4	<0.001
Left bundle branch block	598 (63.2%)	456 (87.5%)	142 (33.4%)	<0.001
Right bundle branch block	119 (12.8%)	0 (0%)	119 (28.2%)	<0.001
Non-specific intraventricular conduction delay	229 (23.6%)	65 (11.3%)	164 (38.6%)	<0.001
Laboratory				
Serum creatinine (mg/dL)	1.1 [0.9,1.5]	1.0 [0.9,1.3]	1.2 [0.9,1.7]	<0.001
White blood cell count (10^9 cells/L)	7.6±2.5	7.5±2.4	7.6±2.6	0.57
Hemoglobin (g/dL)	12.5±2.0	12.7±1.9	12.3±21	0.007
Pharmacotherapy				
Beta-blocker	708 (86.7%)	397 (90.0%)	311 (82.7%)	0.003

	Entire cohort (*n*=946)	QRS PCA Group 1 (*n*=521)	QRS PCA Group 2 (*n*=425)	p
Angiotensin converting enzyme inhibitor or angiotensin-receptor blocker	644 (78.8%)	361 (81.9%)	283 (75.3%)	0.027
Diuretic	625 (76.5%)	334 (75.7%)	291 (77.4%)	0.64
Nitrate	201 (24.6%)	90 (20.4%)	111 (29.6%)	0.003
Hydralazine	94 (11.5%)	45 (10.2%)	49 (13.1%)	0.24
Aldosterone antagonist	282 (34.6%)	151 (34.2%)	131 (34.9%)	0.89
Statin	470 (57.6%)	235 (53.3%)	235 (62.7%)	0.009
Warfarin	236 (28.9%)	104 (23.6%)	132 (35.2%)	<0.001
Clopidogrel	116 (14.2%)	59 (13.4%)	57 (15.2%)	0.52
Digoxin	266 (32.6%)	137 (31.1%)	129 (34.4%)	0.35
Antiarrhythmic	130 (15.9%)	51 (11.6%)	79 (21.1%)	<0.001
Aspirin	536 (65.6%)	287 (65.1%)	249 (66.2%)	0.80

Normally distributed variables reported as mean±SD. Non-normally distributed variables reported as median [25^{th},75^{th} percentile]. Categorical variables reported as *n* (%). PCA=principal components analysis. NYHA=New York Heart Association. LVEF=left ventricular ejection fraction. LVEDD=left ventricular end-diastolic diameter. LVESD=left ventricular end-systolic diameter.

Table 2.

Primary outcomes in subgroups of the study population: (1) Cox proportional hazards model for death, heart transplantation, or LVAD, and (2) LVEF change

	Composite endpoint univariable hazard ratio [95% CI]	p	Mean LVEF change (%) (mean±SD)	p
Entire cohort (*n*=946)				
QRS PCA Group 2 (*n*=425) vs. QRS PCA Group 1 (*n*=521)	0.45 [0.38–0.53]	<0.001	4.8±9.7 vs. 11.1±11.7	<0.001
Non-LBBB (*n*=348) vs. LBBB (*n*=598)	0.52 [0.44–0.62]	<0.001	3.5±9.8 vs. 10.8±11.3	<0.001
QRS area ≤95 (*n*=404) vs. QRS area >95 (*n*=542)	0.46 [0.39–0.55]	<0.001	4.7±10.0 vs. 11.0±11.6	<0.001
LBBB (*n*=598)				
QRS PCA Group 2 (*n*=142) vs. QRS PCA Group 1 (*n*=456)	0.41 [0.32–0.53]	<0.001	6.5±8.9 vs. 12.1±11.6	<0.001
QRSd <150 (*n*=165) vs. QRSd ≥150 (*n*=433)	0.78 [0.6–1.01]	0.058	9.0±11.0 vs. 11.5±11.4	<0.001
QRS area ≤95 (*n*=133) vs. QRS area >95 (*n*=465)	0.42 [0.33–0.55]	<0.001	6.6±9.7 vs. 12.0±11.5	<0.001
LBBB and QRSd ≥150 (*n*=433)				
QRS PCA Group 2 (*n*=87) vs. QRS PCA Group 1 (*n*=346)	0.42 [0.30–0.57]	<0.001	7.3±8.1 vs. 12.5±11.8	0.001
QRS area ≤95 (*n*=56) vs. QRS area >95 (*n*=377)	0.41 [0.28–0.59]	<0.001	8.0±9.6 vs. 12.0±11.6	0.039
Non-LBBB (*n*=348)				
QRS PCA Group 2 (*n*=283) vs. QRS PCA Group 1 (*n*=65)	0.79 [0.57–1.12]	0.18	3.8±10.1 vs. 2.0±8.4	0.32
QRSd <150 (*n*=197) vs. QRSd ≥150 (*n*=151)	0.86 [0.67–1.11]	0.25	2.5±9.5 vs. 5.0±10.1	0.079
QRS area ≤95 (*n*=271) vs. QRS area >95 (*n*=77)	0.80 [0.59–1.09]	0.16	3.6±10.0 vs. 3.2±9.4	0.83
QRSd <150 (*n*=362)				
QRS PCA Group 2 (*n*=201) vs. QRS PCA Group 1 (*n*=161)	0.48 [0.36–0.63]	<0.001	3.4±9.9 vs. 8.5±11.1	<0.001
Non-LBBB (*n*=197) vs. LBBB (*n*=165)	0.58 [0.44–0.76]	<0.001	2.5±9.5 vs. 9.0±11.0	<0.001
QRS area ≤95 (*n*=246) vs. QRS area >95 (*n*=116)	0.50 [0.36–0.68]	<0.001	3.9±9.7 vs. 9.1±11.7	<0.001
QRS PCA Group 1 (*n*=521)				
Non-LBBB (*n*=65) vs. LBBB (*n*=456)	0.49 [0.35–0.69]	<0.001	2.0±8.4 vs. 12.1±11.6	<0.001
QRS area ≤95 (*n*=79) vs. QRS area >95 (*n*=442)	0.64 [0.45–0.91]	0.013	8.1±10.4 vs. 11.7±11.9	0.042
QRS PCA Group 2 (*n*=425)				
Non-LBBB (*n*=283) vs. LBBB (*n*=142)	0.94 [0.74–1.2]	0.63	3.8±10.1 vs. 6.5±8.9	0.036
QRS area ≤95 (*n*=325) vs. QRS area >95 (*n*=100)	0.65 [0.48–0.86]	0.003	3.8±9.7 vs. 7.9±9.4	0.003

	Composite endpoint univariable hazard ratio [95% CI]	p	Mean LVEF change (%) (mean±SD)	p
QRS area >95 (*n*=542)				
Non-LBBB (*n*=77) vs. LBBB (*n*=465)	0.48 [0.35–0.66]	<0.001	3.2±9.4 vs. 12.0±11.5	<0.001
QRS PCA Group 2 (*n*=53) vs. QRS PCA Group 1 (*n*=262)	0.58 [0.43–0.78]	<0.001	7.9±9.4 vs. 11.7±11.9	0.018
QRS area ≤95 (*n*=404)				
Non-LBBB (*n*=271) vs. LBBB (*n*=133)	0.93 [0.72–1.20]	0.55	3.6±10.0 vs. 6.6±9.7	0.021
QRS PCA Group 2 (*n*=325) vs. QRS PCA Group 1 (*n*=79)	0.59 [0.42–0.83]	0.002	3.8±9.7 vs. 8.1±10.4	0.005

QRSd units in ms. QRS area units in μVs. LVAD=left ventricular assist device. LVEF=left ventricular ejection fraction. CI=confidence interval. SD=standard deviation. LBBB=left bundle branch block. PCA=principal components analysis.